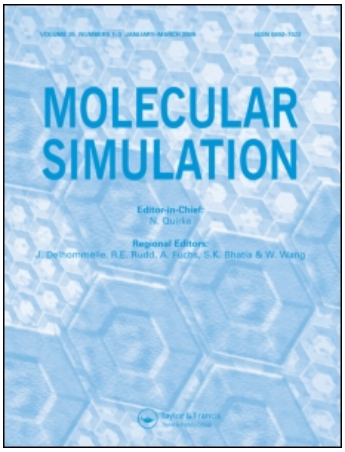

Molecular Simulation
Publication details, including instructions for authors and subscription information:
http://www.informaworld.com/smpp/title~content=t713644482

Molecular Dynamics Simulation for the Mixture of Water and an Ice Nucleus

T. Yokoyama[a]; Y. Hagiwara[a]
[a] Department of Mechanical and System Engineering, Kyoto Institute of Technology, Kyoto, Japan

Online publication date: 26 October 2010

To cite this Article Yokoyama, T. and Hagiwara, Y.(2003) 'Molecular Dynamics Simulation for the Mixture of Water and an Ice Nucleus', Molecular Simulation, 29: 4, 235 — 248
To link to this Article: DOI: 10.1080/0892702031000065584
URL: http://dx.doi.org/10.1080/0892702031000065584

Molecular Simulation, 2003 Vol. 29 (4), pp. 235–248

Molecular Dynamics Simulation for the Mixture of Water and an Ice Nucleus

T. YOKOYAMA and Y. HAGIWARA

Department of Mechanical and System Engineering, Kyoto Institute of Technology, Goshokaido-cho, Matsugasaki, Sakyo-ku, Kyoto 606-8585, Japan

(Received July 2002; In final form October 2002)

We have carried out a molecular dynamics simulation for the melting and solidification of ice nucleus. An ice crystal was formed by controlling the displacement and velocity of each molecule. Part of the ice was melted by supplying energy to it in order to produce a mixture of an ice nucleus and surrounding water at approximately freezing point. By using this mixture, a mixture of an ice nucleus and supercooled water was made. It was found that the time scale for the correlation between the potential energy and the rotational component of the kinetic energy was different from that of the correlation between the potential energy and the translational component of the kinetic energy. Also, it was predicted that the ice nucleus received forces whose directions were not exactly the same as those of the growth of ice crystal.

Keywords: Ice crystal; Ih structure; Melting; Solidification; Supercooled water

INTRODUCTION

There is a growing interest in the control of ice growth in ice–water mixture. The control of ice growth is one of the key technologies for the storage of food and the storage of internal organs in hospitals. Various methods have been proposed to improve this process. Among the methods, some additives for the mixture, such as proteins, fibers and silane coupling agents, have recently been focused on. It was found from the observation of these additives by scanning tunneling microscope that the additives form the grooves at a specific location for a tiny ice crystal [1,2]. However, the mechanism of the interaction between the ice crystal and the additives has not yet been fully understood.

In order to understand the ice growth phenomenon in ice–water mixture, Haymet and co-workers carried out molecular dynamics simulations [3–5]. They developed a reliable method for obtaining the interface between water and specific planes in the hexagonal prism of ice crystal. Their results and discussion are useful. However, their method, in which the box of molecules for the ice crystal and the box of water molecules are joined in order to make an interface, is not directly applicable for realizing a tiny ice cube surrounded by water. This kind of ice crystal is useful not only for examining how it grows but also for reducing the effect of the boundary of computational domain on the ice–water interface. Although Svishchev and Kusalik [6] formed a cubic ice nucleus with Ic structure, they did not study the nucleus with Ih structure. Therefore, these studies give no clarification on how to deal with the interface between water and an ice nucleus with Ih structure. As far as the present authors know, no other works have been done for the three-dimensional ice nucleus in water.

It should be noted that Dalal *et al.* [7] investigated the effect of antifreeze protein on the interface of water and ice crystal with a specific plane in detail. They found that hydrogen bonding is not the primary reason for the interaction. It is worthwhile to investigate the interaction between the ice nucleus and the amino acids in antifreeze protein.

This study aims at elucidating the interaction between the ice nucleus and surrounding water with a molecular dynamics simulation. The ice nucleus with Ih structure is obtained by gradual relaxation of the molecules in non-equilibrium state in the simulation. Water surrounding the ice is also obtained from the ice crystal in a similar manner. The goal of the present authors' research is to clarify the key parameters for the interaction between ice nuclei and antifreeze proteins by using the molecular dynamics simulation.

ISSN 0892-7022 print/ISSN 1029-0435 online © 2003 Taylor & Francis Ltd
DOI: 10.1080/0892702031000065584

METHODS FOR MOLECULAR DYNAMICS SIMULATION

The classical molecular dynamics simulation was applied in this study. It was assumed that the number of molecules, the volume of computational domain and the total energy were kept constant (hereafter called the *NVE* ensemble) except for heating or energy removal procedures, in which we changed only the energy, mentioned below. The molecules were assumed as solid bodies. The Newton–Euler equations for the translational and rotational motions were solved at each time step. The dipole moment, which was discussed by Hayward and Reimers [8], was not evaluated in the present study.

Potential Functions

The TIP4P potential [9] was adopted for the potential function for the interaction between two water molecules. This potential has better accuracy compared with the other potential for water. The potential function consists of the Coulomb potential and the Lennard–Jones potential.

The cutoff of the force acting on two distant molecules was done with the two following methods: the cutoff radius for the Lennard–Jones potential and the Ewald method [10] for the Coulomb potential. The cutoff radius was set at 2.245 nm, which is equal to the dimension of the ice nucleus in the x-direction. The parameters for the Ewald summation were $\alpha = 5.6$, $|\mathbf{u}_x|_{\max} = 1$, $|\mathbf{h}_x|_{\max} = 5$ where α is the width of the Gaussian distribution, $\mathbf{u}_x$ is the vector for the location of image cell in the x-direction in the physical space and $\mathbf{h}_x$ is the vector for the location of image cell in the Fourier space.

Time Integral

The Newton–Euler equations for the translational and rotational motions were integrated with the Gear algorism [11], a one-step predictor–corrector method. We adopted 5-value Gear algorism in which the time derivatives up to the fifth order are considered for the second-order differential Newton–Euler equation for the translational motion. We also used 4-value Gear algorism for the second-order differential Newton–Euler equation for the rotation. All the computations were carried out with the time step of 0.5 fs.

Estimation and Adjustment of Temperature

The statistical temperature, T, was given with the law of equi-partition of energy by the total energy of the translational motion for all the molecules, K_{T}, and that of the rotational motion for the molecules, K_{R}. The temperature is written as follows:

$$\begin{aligned} T &= \frac{1}{2}\left(\frac{2}{3k_{\mathrm{B}}N}K_{\mathrm{T}} + \frac{2}{3k_{\mathrm{B}}N}K_{\mathrm{R}}\right) \\ &= \frac{1}{3k_{\mathrm{B}}N}\left\{\frac{1}{2}\sum_{i=1}^{N} m\mathbf{v}_i^2 + \frac{1}{2}\sum_{i=1}^{N}\left(I_{px_i}\omega_{px_i}{}^2\right.\right. \\ &\quad \left.\left. + I_{py_i}\omega_{py_i}{}^2 + I_{pz_i}\omega_{pz_i}{}^2\right)\right\} \end{aligned} \tag{1}$$

where k_{B} is the Boltzmann constant, N is the total number of molecules, m is the mass of molecules, I_p is the inertia based on its principal axis. The temperature scaling was done by changing the translational velocity, $\mathbf{v}$, and the angular velocity, ω, of each molecule with the following equation:

$$\mathbf{v}_i^{(\mathrm{new})} = \mathbf{v}_i^{(\mathrm{old})}\sqrt{\frac{T_{pd}}{T_0}}, \quad \omega_i^{(\mathrm{new})} = \omega_i^{(\mathrm{old})}\sqrt{\frac{T_{pd}}{T_0}}. \tag{2}$$

Self-diffusion Coefficient

The self-diffusion coefficient can be calculated by the following equation:

$$D = \lim_{t\to\infty}\frac{1}{6t}\frac{1}{N}\sum_{i=1}^{N}(\boldsymbol{r}_i(t) - \boldsymbol{r}_i(0))^2, \tag{3}$$

where $\boldsymbol{r}_i(t)$ is the coordinate of a molecule i at time t. The function defined by the following equation, which is derived from Eq. (3), was used for judging the state of system:

$$D(t) = \frac{1}{N}\sum_{i=1}^{N}(\boldsymbol{r}_i(t) - \boldsymbol{r}_i(0))^2. \tag{4}$$

If the function (hereafter called diffusion function) increases with time, the system is in a liquid state. On the other hand if the diffusion function does not change in time, the system remains in a solid state.

Radial Distribution Function

The radial distribution function of oxygen atoms for a specific oxygen atom (hereafter called O–O radial distribution function) was used for examining whether or not the ice has a crystal structure. The function is expressed as follows [12]:

$$g(r) = \frac{V}{N^2}\left\langle\sum_i\sum_{j\neq i}\delta(\boldsymbol{r}_i - \boldsymbol{r}_j)\right\rangle, \tag{5}$$

where $\boldsymbol{r} = |\boldsymbol{r}_i - \boldsymbol{r}_j|$ is the distance between two oxygen atoms, V is the volume of computational

domain and N is the number of oxygen atoms. In the case of ice–water mixture, we used the following function with a conditional sampling:

$$g(r) = \frac{V^*}{N^{*2}} \left\langle \sum_i \sum_{j \neq i} \delta(\boldsymbol{r}_i^* - \boldsymbol{r}_j^*) \right\rangle, \qquad (6)$$

where * denotes that only the atoms in water are considered to calculate the function for water, and that only the atoms in ice are considered to calculate the function for ice.

COMPUTATIONAL PROCEDURE

In order to obtain a mixture of water and a tiny ice crystal, the following three methods can be considered: (1) the ice crystal and water are made independently then they are put into the computational domain, (2) the water is filled in the whole domain first, then the energy for a small part of the domain is reduced to form the ice crystal in this sub-domain, and (3) the ice is filled in the whole domain first, then the energy for most of the domain is increased to melt the ice. The inconsistency of the energies of each molecule is the highest for the first method, and thus the computation may fail at the mixing instant. As far as the present authors know, there is no established technique how to settle the molecules in water to the positions of Ih structure associated with the second method. Therefore, we selected the third method for the present study. In order to obtain the mixture of supercooled water and ice nucleus, we developed three successive procedures for the method explained in the following.

Formation of Ice

An approximately cubic domain was given in the Cartesian coordinate. The initial arrangement of the molecules was determined with the results obtained in the previous studies [3,8,13,14]. Sixty molecules were positioned so that the center of mass for each molecule was on a plane normal to the z-axis, and six planes were considered in the domain. Hence, the directions of crystal growth are the x- and y-directions. On the other hand, the rotational angle for each molecule at the initial state was given randomly, thus the orientation of hydrogen atom was completely random. The computational condition is shown in Table I.

The Newton–Euler equations for the translational and rotational motions were solved at each time step with the following constraint conditions.

1. The displacement of each molecule calculated from the velocity and the time step was reduced to 0.1% of its value. Under this constraint condition for the displacement, the temperature scaling was done at every time step for 5 ps.
2. Then, the constraint condition for the location of each molecule was stopped. The computation continued only with the temperature scaling at every time step for the next 20 ps.
3. After the adjustment terminated, further computations were carried out without the temperature scaling for 50 ps in order to evaluate the diffusion function and the O–O radial distribution function.

The computation was carried out at the given temperatures of 255, 260, 265, 285, 290 and 300 K.

Production of Ice–water Mixture

The new computational domain whose dimension was twice as large as that used above in the three directions was filled with eight identical ice crystals. The crystals were the same as that obtained above for 265 K. This is the initial state for the procedure of producing an ice–water mixture. Only one of the crystals, which was located near a lower corner of the domain, was used as the ice nucleus, and the rest was melted by heating and used for water region. The computational condition is shown in Table II.

Before the heating, the computation was carried out for 5 ps (0–5 ps), in which the locations of 360 molecules in the region for the ice nucleus were constrained, while the locations of the other molecules in the water region were not constrained.

All the molecules in the liquid region were heated gradually by using the following steps:

1. The temperature scaling was applied instantaneously only for the translational velocity of each molecule in the water region.

TABLE I Computational condition for forming ice nucleus

Domain size (nm^3)	2.245 × 2.333 × 2.200
Number of molecules	360
Minimum distance for centers of mass of two molecules (nm)	0.275
Density ($g\,cm^{-3}$)	0.934

TABLE II Computational condition for producing ice–water mixture

Domain size (nm^3)	4.491 × 4.667 × 4.400
Number of molecules for ice nucleus	360
Number of molecules for liquid region	2520
Total number of molecules	2880
Initial temperature (K)	265
Ice nucleus temperature (K)	265
Target temperature for melting (K)	300

TABLE III Mean values of potential energy, molecular translational temperature and molecular rotational temperature for ice and water

	Ice nucleus	Liquid region
Potential energy (kJ mol^{-1})	−48.0	−42.9
Translational kinetic energy (kJ mol^{-1})	3.27*	3.44
Translational temperature (K)	262.6	276.2
Rotational kinetic energy (kJ mol^{-1})	3.29*	3.45
Rotational temperature (K)	264.0	276.9

*The results of ice nucleus for 50 ps.

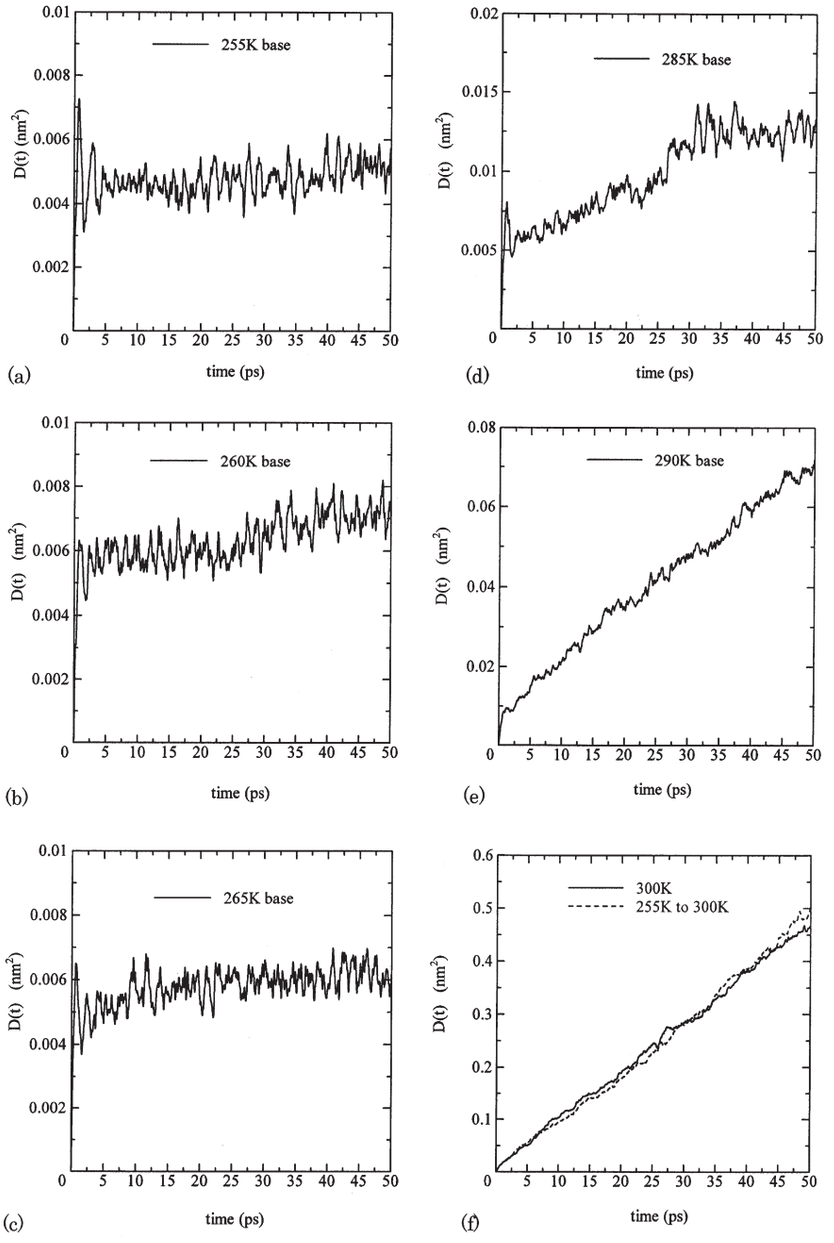

FIGURE 1 Time changes in diffusion function for ice (a) 255 K, (b) 260 K, (c) 265 K, (d) 285 K, (e) 290 K, (f) 300 K.

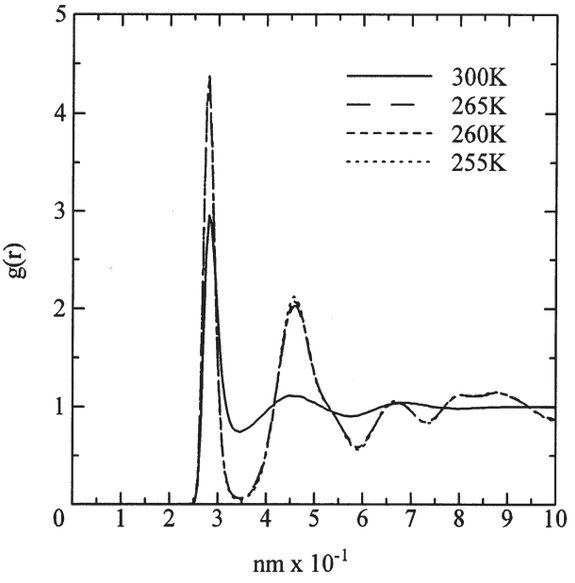

FIGURE 2 O–O radial distribution function of ice.

2. Then, the computation was carried out without the temperature scaling for 50 fs.
3. The procedures 1 and 2 were repeated 100 times in the period of 5 ps.
4. Further computation was carried out for the relaxation of temperature and energy in the whole computational domain for the next 5 ps. The temperature scaling was not applied at all during this procedure.
5. The predetermined temperature of the water region was increased by 2 K.
6. The procedures from 1 to 5 were repeated until the predetermined temperature was equal to a target temperature.

   The target temperature was set at 300 K. This temperature is associated with the latent heat of melting, which is discussed below. One hundred and eighty picoseconds (5–185 ps) were spent for the heating. Notwithstanding the heating, the diffusion function and the O–O radial distribution function were found to be similar to the counterparts of ice (figure omitted). Therefore, the following two procedures were carried out.
7. The same procedure as that mentioned above in 2 was done keeping the temperature at 300 K for 50 ps (185–235 ps).
8. Finally, the computation was carried out without the temperature scaling for 170 ps (235–405 ps). The interaction of all the molecules was calculated.

Note that the positions of molecules in the ice nucleus were constrained, while the positions of molecules in the water region were not constrained throughout the heating procedures. This constraint of molecules terminated after the heating procedures were completed.

Mixture of Ice and Supercooled Water

We used the final results calculated by the production procedure of the ice–water mixture as the initial condition for the computation to obtain the mixture of supercooled water and ice. As is shown in Table III, the mean potential energy for the liquid region of ice–water mixture was much higher than that of ice. Thus, we should remove the energy from the liquid region in order to obtain the supercooled water. We adopted the following steps for the energy removal:

1. The temperature scaling was applied instantaneously only for the translational velocity of each molecule in the water.
2. Then, the computation was carried out without the temperature scaling for 50 fs.
3. The procedures 1 and 2 were repeated 100 times in the period of 5 ps.
4. The predetermined temperature of the water region was decreased by 2 K.
5. The procedures from 1 to 4 were repeated until the predetermined temperature was equal to a target temperature.

The target temperature was set at 240 K. This temperature is also associated with the latent heat, which is discussed below. Ninety picoseconds (5–95 ps) were spent for the energy removal. Note that the positions of molecules in the ice nucleus were constrained, while the positions of molecules in the water region were not constrained throughout the energy removal procedures. This constraint of molecules terminated after the energy removal procedures were completed.

RESULTS AND DISCUSSION

Ice Nucleus

The result for 50 ps after stopping the constraint condition was examined with the diffusion function, the O–O radial distribution function and snapshots.

Diffusion Function

Figure 1 shows the diffusion function for each case. The function in the case where the ice Ih made at 255 K was heated until 300 K and kept its temperature is also demonstrated in Fig. 1(f). Although the function fluctuates with time, the average values of the coefficients in Figs. 1(a)–(c) seem nearly constant

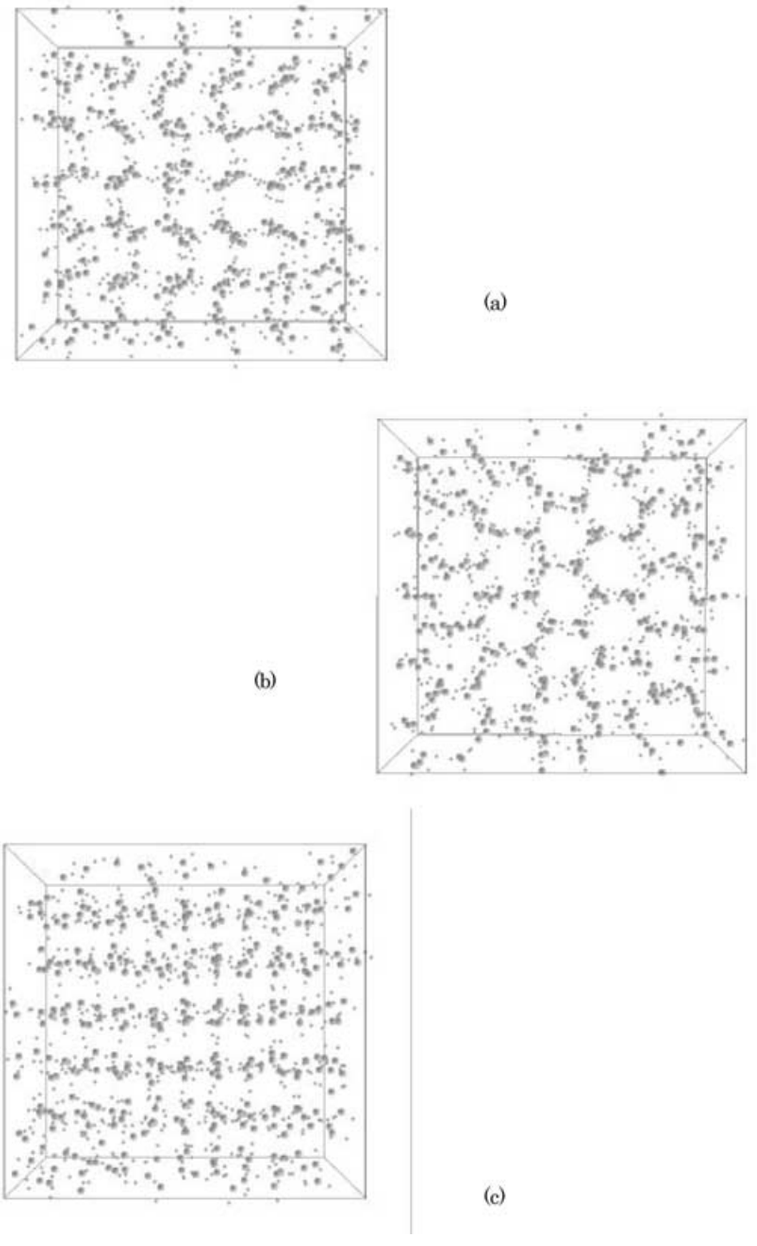

FIGURE 3 Snapshot of molecules in ice at 265 K (a) view from *x*-axis, (b) view from *z*-axis, (c) view from *y*-axis.

with time in cases at 255, 260 and 265 K. It can be considered that the molecules are in the solid state in these three cases.

On the other hand, the functions in the cases of 285, 290 and 300 K increase with time. The increasing rate becomes higher than those in the cases of lower temperature than 265 K. These show that the molecules are not in a solid state.

The self-diffusion coefficient was estimated to be $1.6 \times 10^9\ m^2\ s^{-1}$ from Fig. 1(f) and Eq. (3). This is lower than the experimental result at 300 K, and is nearly equal to that at 283 K [15]. Considering the density of the ice shown in Table I, which is slightly higher than that in the experiment, the present value of the coefficient is reasonable. It can be concluded from the above mentioned results that the molecules are in a solid state in cases lower than 265 K.

TABLE IV Comparison of mean temperature in the liquid region with the predetermined temperature

Elapsed time (ps)	55	105	155	185
Predetermined temperature (K)	275	285	295	300
Mean temperature in liquid region (K)	277.0	283.9	293.4	299.6

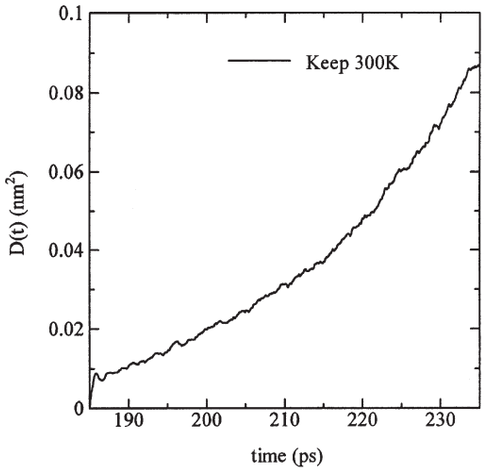

FIGURE 4 Time change in diffusion function for the period of 185–235 ps.

Radial Distribution Function

The O–O radial distribution function was evaluated from the locations of molecules at every 5 fs. Figure 2 shows the function at 255, 260, 265 and 300 K. The minimum between the first and second peaks is not clear and the function takes nearly unity at around $r = 0.7$ nm in case of 300 K. This is in qualitative agreement with the experimental result for water at the same temperature [9]. On the other hand, not only the minimum but also these peaks and even the third and fourth peaks are noticeable in the other cases. This confirms an existence of an ordered structure under 265 K.

Snapshots

It is found from the above mentioned discussion that the solid ice was realized for the temperature lower than 265 K. In order to confirm that the ice has the Ih structure, we observed the visualized molecules at some moments. Figure 3 shows a snapshot of molecules from three different viewpoints at 265 K. Clear hexagonal structure is seen in the whole computational domain in Fig. 3(b), which is different from the structure observed in the ice in the amorphous state. Figure 3(a) resembles the model structure of ice Ih. Therefore, we concluded that the ice obtained by the present computation in the cases of temperatures lower than 265 K is in the ice Ih crystal state.

Ice–water Mixture

Table IV shows the comparison of mean temperature in the liquid region with the predetermined temperature. The mean temperature seems to cover to the final predetermined temperature of 300 K at the final moment (185 ps). However, the diffusion function was found to still increase with time for the final period (figure omitted). Furthermore, the O–O radial distribution function indicated much higher peaks and deeper valleys than those of water at 300 K (figure omitted). The total energy input until this moment was much lower than the latent heat of melting of ice at the atmospheric pressure, which is 333 kJ kg^{-1}. Therefore, the period of 10 ps was not enough to melt the ice in the liquid region completely.

Then, we continued the heating for a further 50 ps with the predetermined temperature of 300 K. Figure 4 demonstrates that the diffusion function increases overall for the continuous heating. The increasing rate of the diffusion function for the final 2 ps is much lower than that for most of the other periods. We confirmed that the increasing rate became still lower if the computation continued.

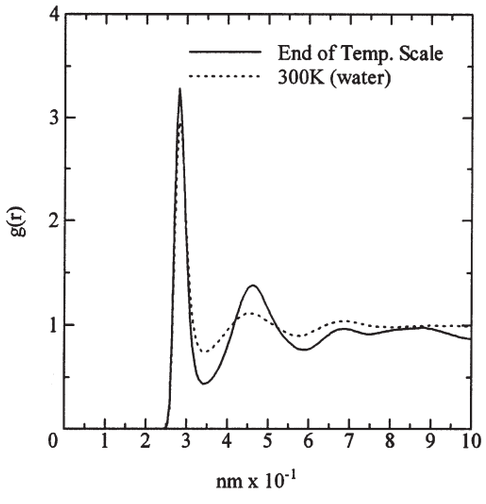

FIGURE 5 O–O radial distribution function for the period of 225–235 ps.

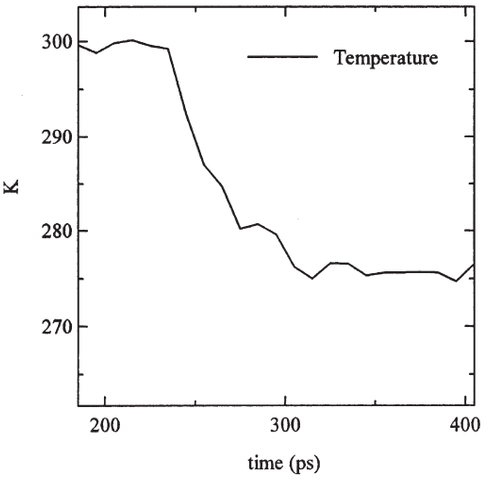

FIGURE 6 Time change in the mean temperature after 185 ps.

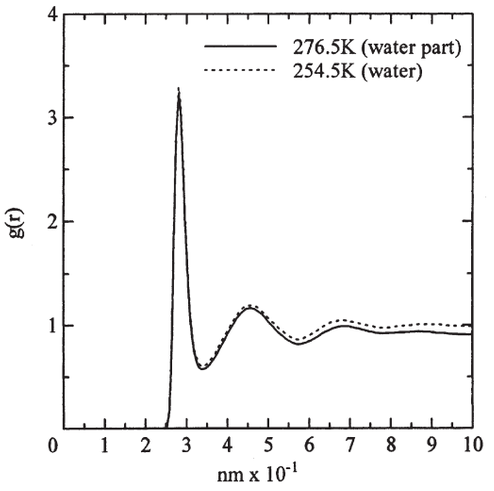

FIGURE 7 O–O radial distribution function for the period of 395–405 ps.

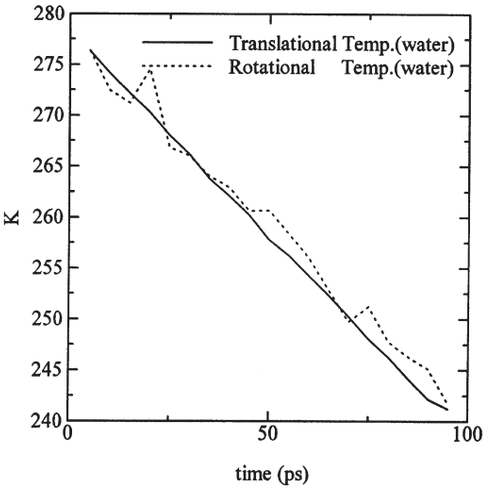

FIGURE 8 Time changes in the molecular translational temperature and rotational temperature for cooling period of water.

The O–O radial distribution function for the final 10 ps is shown in Fig. 5. The distribution function for the final 10 ps is closer to that of the water at 300 K than the function for any other period. The total energy input was approximately 90% of the latent heat. Therefore, we concluded that the molecules in the liquid region after the heating for 50 ps are in a liquid state at 235 ps and the heating was then terminated. Note that the lower target temperature can be selected. In this case, however, it takes more time to input energy approximately equal to the latent heat with the scaling procedure.

Figure 6 indicates the mean temperature for the liquid region as a function of time after 185 ps. The temperature was kept at approximately 300 K through the final heating for 50 ps. Then the interaction between the molecules in the liquid region and those in the ice was considered. The temperature decreased rapidly soon after this consideration of the interaction. The temperature remained in a stable state at approximately 275 K after 300 ps. The O–O radial distribution function in the liquid region for 395–405 ps is drawn in Fig. 7. The broken line in this figure is the distribution function for water at 275 K, which was obtained by cooling the single-phase water at 300 K shown in Fig. 1(f) gradually. These two functions resemble each other. The structure of the ice was not changed by this interaction. Therefore, we concluded that we obtained the mixture of water and ice nucleus as a consequence of the above mentioned procedures.

TABLE V Mean values of potential energy, molecular translational temperature and molecular rotational temperature for the mixture of ice and supercooled water

Potential energy (kJ mol^{-1})	−45.1
Translational temperature (K)	240.2
Rotational temperature (K)	240.7

Mixture of Ice and Supercooled Water

Energy Removal from Water

Table III shows the average potential energy and the kinetic energy obtained by the procedure in the period of 395–405 ps. This table indicates that energies in the liquid region are higher than those of the ice nucleus. This is the reason for the above mentioned energy removal procedure.

Figure 8 depicts the change in the mean temperature for the energy removal procedure for

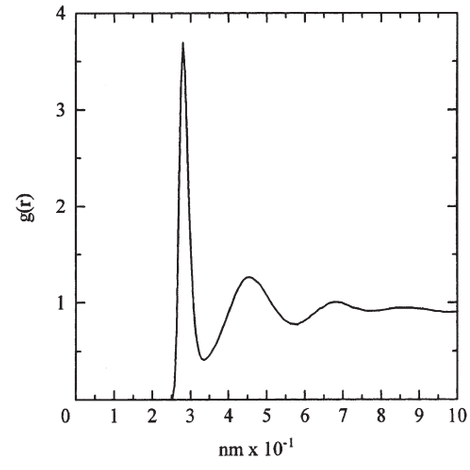

FIGURE 9 O–O radial distribution function for the final 5 ps in cooling period.

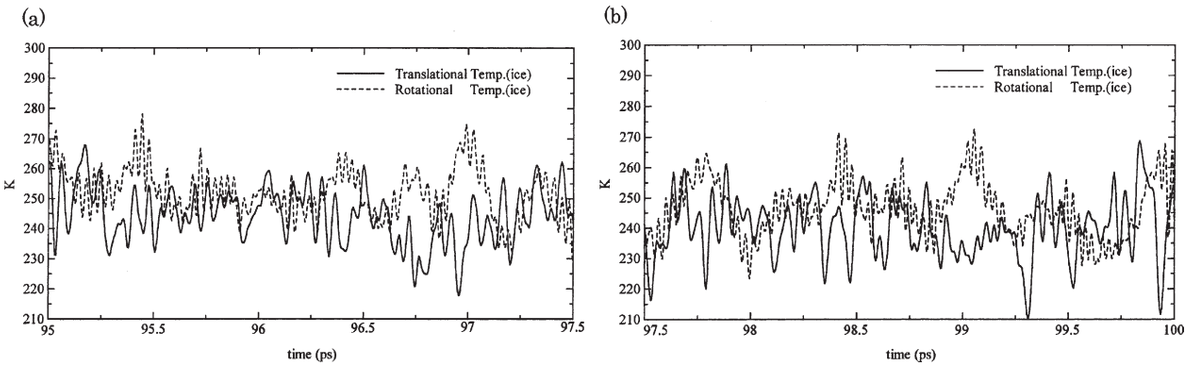

FIGURE 10 Time changes in the molecular translational temperature and rotational temperature of ice (a) 95–97.5 ps, (b) 97.5–100 ps.

95 ps. The location of each molecule in the ice was fixed through this procedure. The solid and broken lines show the translational and rotational temperatures of water, respectively. These temperatures are found to decrease almost linearly to 240 K.

The mean values of the potential energy, the translational temperature and the rotational temperature for the final period of the procedure (90–95 ps) are shown in Table V. The mean potential energy is found to be lower than that of water at 276 K and closer to that of ice. Figure 9 shows the O–O radial distribution function for the period. This function is similar to that of water at 276.5 K shown in Fig. 7. It is confirmed from this figure that the liquid state was held through the cooling procedures. Therefore, it was concluded that supercooled water at 240 K was realized by this procedure.

The total energy removed was 161 kJ kg^{-1}. This is approximately 50% of the latent heat. Note that further removal of energy may cause quick freezing. Furthermore, the removal of a much smaller amount of energy than that in this case by using higher target temperature is not sufficient for making supercooled water.

Release from the Supercooled State

After the energy removal procedure, the interaction between the ice nucleus and the supercooled water was started. At the beginning of the interaction, the molecular translational temperature of ice changed noticeably. The time changes in the molecular translational temperature and the molecular rotational temperature of the ice and those of the water are demonstrated in Figs. 10 and 11, respectively. It is found from Fig. 10 that the translational temperature for ice quickly approaches the liquid temperature. It is also found from comparing two figures that the temperature fluctuation of ice is always more noticeable than that of the liquid region. The mean temperature for the ice over the 5 ps was 245.8 K and that for the liquid region was 241.0 K.

The continuous interaction between the ice and water lead to a gradual change in the energy. Figure 12 shows time change in the mean potential energy for 100 ps, and Fig. 13 shows time change in the mean temperature for the period. All the lines in these figures are drawn based on the data at every

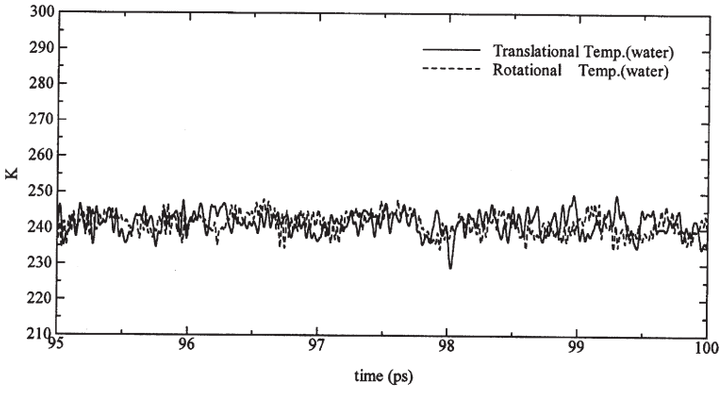

FIGURE 11 Time change in the molecular translational temperature and rotational temperature of water.

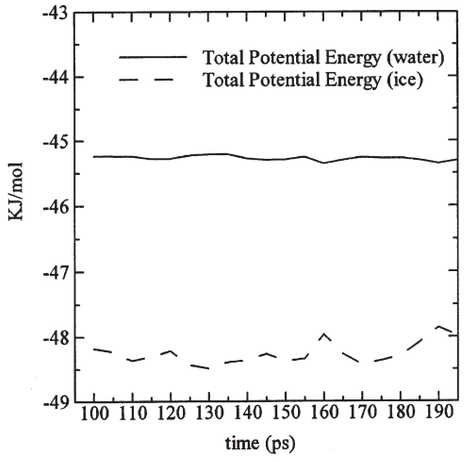

FIGURE 12 Time changes in the mean potential energies of ice and supercooled water.

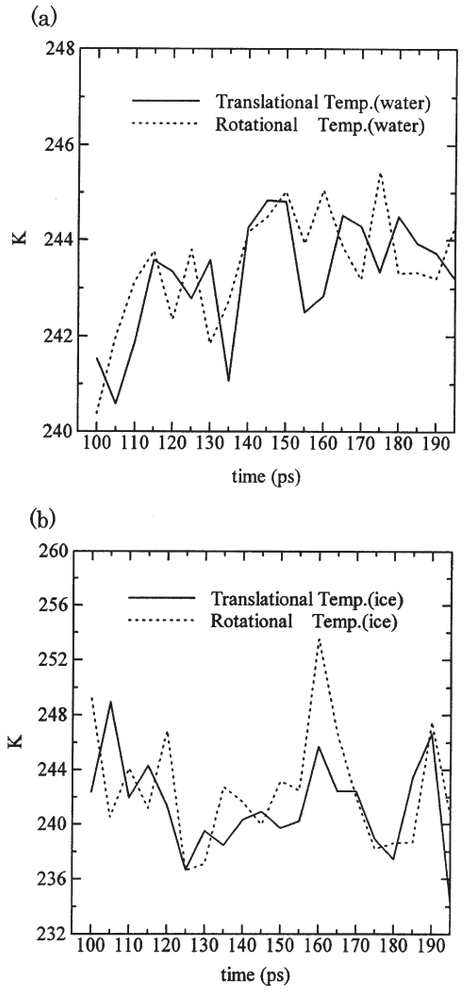

FIGURE 13 Time changes in the mean molecular translational temperature and rotational temperature (a) supercooled water, (b) ice.

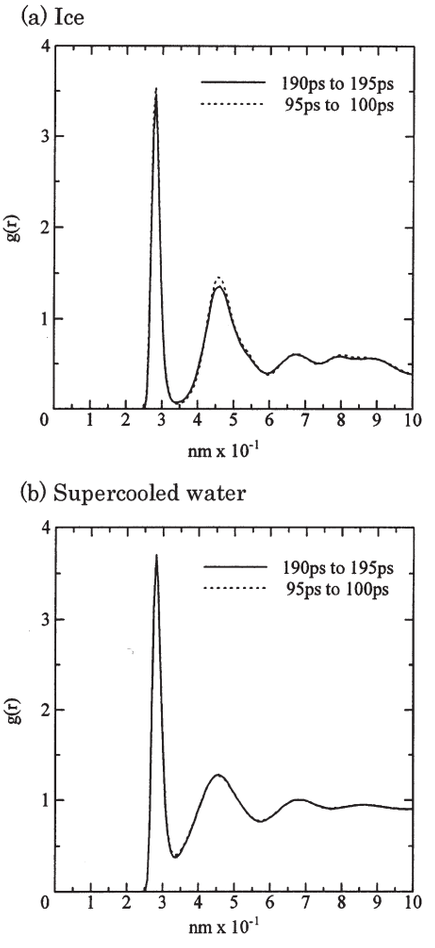

FIGURE 14 Comparison of O–O radial distribution function for the period of 190–195 ps and that of 95–100 ps (a) ice, (b) supercooled water.

5 ps. The slight decrease in the potential energy in the liquid region with time is seen in Fig. 12. The corresponding increase in the temperature is observed in Fig. 13(b). On the other hand, the potential energy of ice increases with time, and the temperature of ice tends to decrease as shown in Fig. 13(a).

Figure 14 shows the O–O radial distribution functions for 95–100 ps and those for 190–195 ps. A decrease in the second maximum is seen for the O–O radial distribution function of ice. Although the mean temperature of the liquid region increases, a decrease in the minimum value of the liquid region is seen. This represents the release of supercooled state due to the local solidification of water near the interface.

When the temperature of the supercooled liquid was set at 260 K, the temperature would not decrease, and the potential energy of the ice nucleus became closer to that of the liquid region. The O–O radial distribution function showed that the ice tends

TABLE VI Mean, standard deviation and skewness for probability density distribution of force

Direction	Statistics	Short period	Long period
x	Average	0.252×10^{-6}	0.185×10^{-6}
	Standard deviation	0.102×10^{-3}	0.984×10^{-4}
	Skewness	0.109	0.55×10^{-1}
y	Average	-0.162×10^{-6}	0.675×10^{-7}
	Standard deviation	0.107×10^{-3}	0.980×10^{-4}
	Skewness	-0.108	-0.435×10^{-1}
z	Average	0.324×10^{-5}	0.689×10^{-7}
	Standard deviation	0.966×10^{-4}	0.903×0^{-4}
	Skewness	-0.282	-0.463×10^{-1}

to melt. Thus, the solidification of water is found not to be enhanced by the existence of the supercooled water and the ice nucleus in the present computation. This is partly because the limited numbers of molecules were considered and partly because the *NVE* ensemble was adopted.

Correlation Between Potential Energy and Kinetic Energy

Figure 15 shows the power spectra of the energy fluctuation for 100 ps. The spectra of the energy fluctuation for ice resemble those for the liquid region. It is found by comparing the spectra that the spectrum of the potential energy has a high correlation to the rotational kinetic energy in the high frequency range of $20-30\,\mathrm{ps}^{-1}$. On the other hand, the spectrum correlates to the translational kinetic velocity in the middle frequency range of $10-20\,\mathrm{ps}^{-1}$. Since the center of the water molecule is closely located to that of the oxygen atom, the rotation of the molecules is caused by the hydrogen atoms. The high frequencies of the energy spectra are considered to express movement of the molecules.

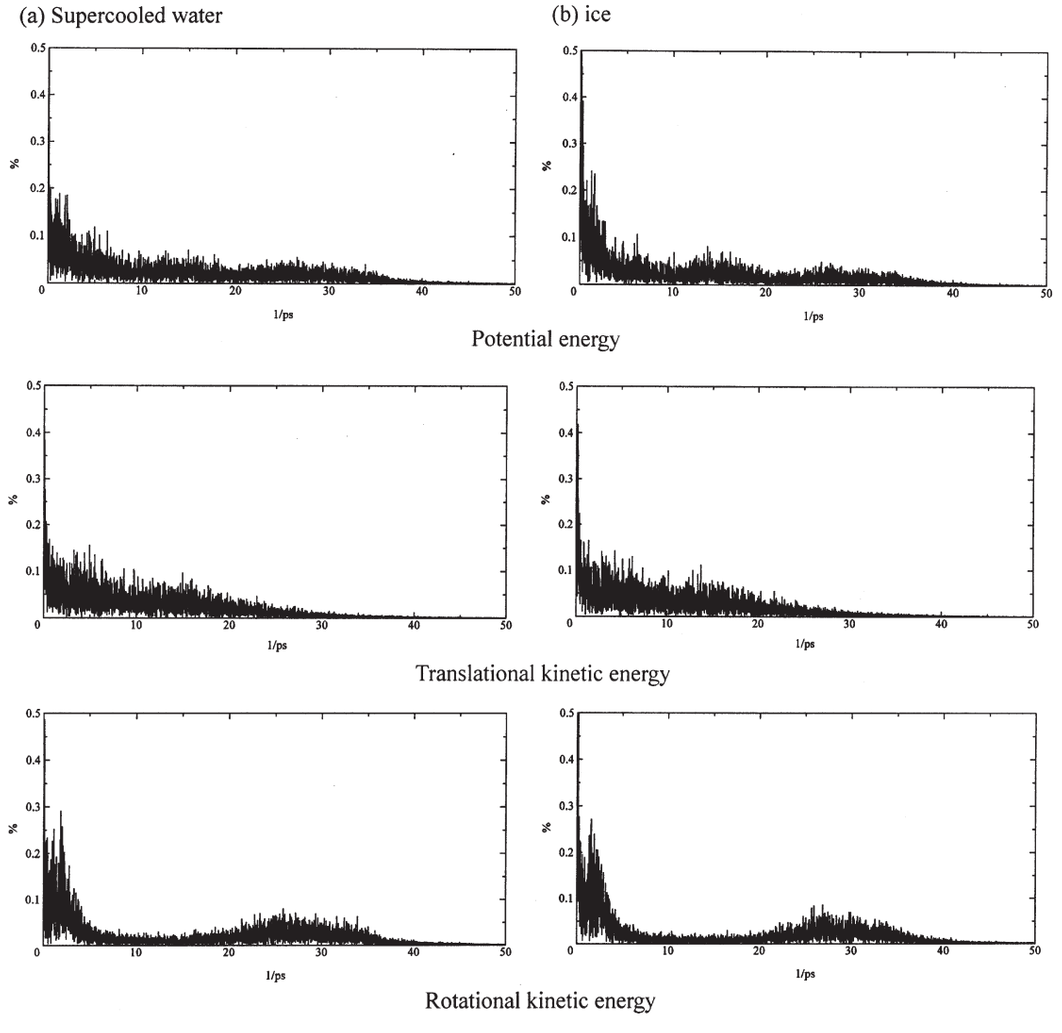

FIGURE 15 Power spectra of the potential energy, the translational kinetic energy and the rotational kinetic energy (a) supercooled water, (b) ice.

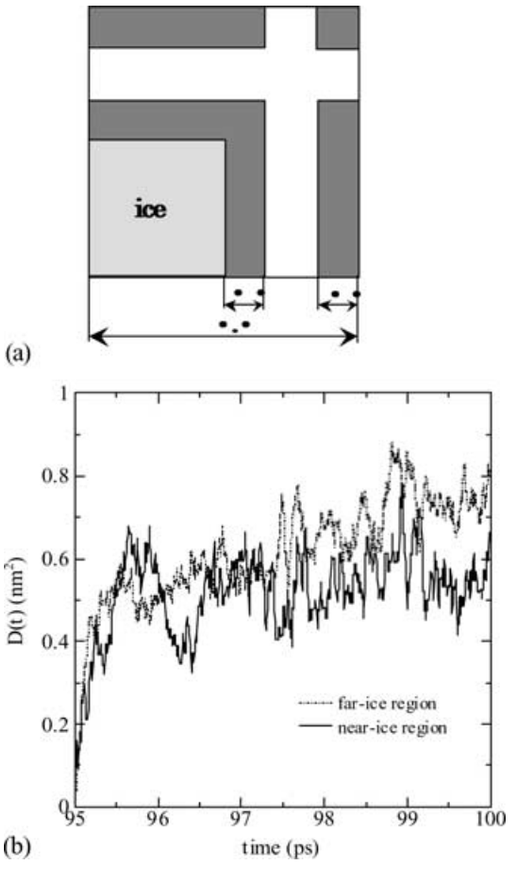

FIGURE 16 Diffusion functions for supercooled water in near-ice region and far-ice region (a) two-dimensional illustration of near-ice regions in gray and far-ice region in white, (b) diffusion functions in these regions.

This is due to the vibration of the hydrogen atoms, which received energy. Then, the accumulated energy generated the translational motion of oxygen and thus the water molecules. This is the reason for the predominant translational energy in the range of $5-20\,\mathrm{ps}^{-1}$. This energy enhances translational motion of the molecules. This motion may lead to the motion of cluster of the water molecules, in which the molecules are weakly connected by the hydrogen bonding. Furthermore, the ice nucleus is deformed as mentioned above. These large-scale motions of molecules cause increases in the translational and rotational energies in the low frequency range. The spectra for the supercooled water are similar to those for the ice nucleus. This is in agreement with the experimental result, in which no qualitative difference was found between the spectrum for water and that for ice [4].

Water Molecules around the Ice Nucleus

In order to examine the effect of the ice nucleus on the water around the nucleus, we divided the water region into two parts: a near-ice region and a far-ice region. The near-ice region was defined by thin layers on the whole surface of the ice nucleus (See Fig. 16(a)). The thickness of the layer, δ, was 0.56 nm. δ was determined arbitrarily and is a quarter of the edge of the nucleus in the x-direction. Although the number of molecules inside this region changed with time, 867 molecules, which was approximately one third of all the water molecules, were inside this region on average through the period of 90–95 ps (just after the energy removal procedure was terminated). Figure 16(b) shows the diffusion function for water molecules. The solid bold line and the dotted line indicate the function for the molecules in the near-ice region and that for the molecules in the far-ice region, respectively. It is found that the function for the molecules in the far-ice region increases with time. On the other hand, the function for the molecules in the near-ice region does not increase with time, though it fluctuates with time. Therefore, the molecules in the near-ice region are basically in the solid state. On the other hand, both the function for the molecules in the near-ice region and that in the far-ice region increased with time for the first 5 ps after the energy removal procedure started (figure omitted). These show that the supercooled water near the ice nucleus is solidifying by the procedure. However, clear hexagonal structure of molecules, such as shown in Fig. 3(b), was not observed for the molecules in the near-ice region. This suggests that even if the molecules in the near-ice region cease diffusing, it takes time for the molecules to form a specific structure. The solidification of water near the interface may be related with the ice-like behavior of molecules in a thin layer near the ice–water interface discovered by Hayward and Haymet [4].

Forces Acting on Ice and Water

We examined the distribution of probability density for the translational force acting on the supercooled water and ice. Figure 17 shows the distribution for 5 ps in the three directions. The distribution of ice is symmetrical to that of water with respect to the ordinate because of the principle of action and reaction. Table VI shows the average, the standard deviation and the skewness of the distributions in Fig. 17. It is found that the ice tends to receive forces in the positive direction of the x-axis and in the negative directions of the y- and z-axes. The absolute value of the skewness in the z-direction is much higher than the other two. The absolute value in the y-direction is the lowest among the three. This means that the force acting on the liquid region or ice nucleus is anisotropic in the period.

Table VI also shows the statistical quantities for 100 ps. Even for this longer period, the ice tends to

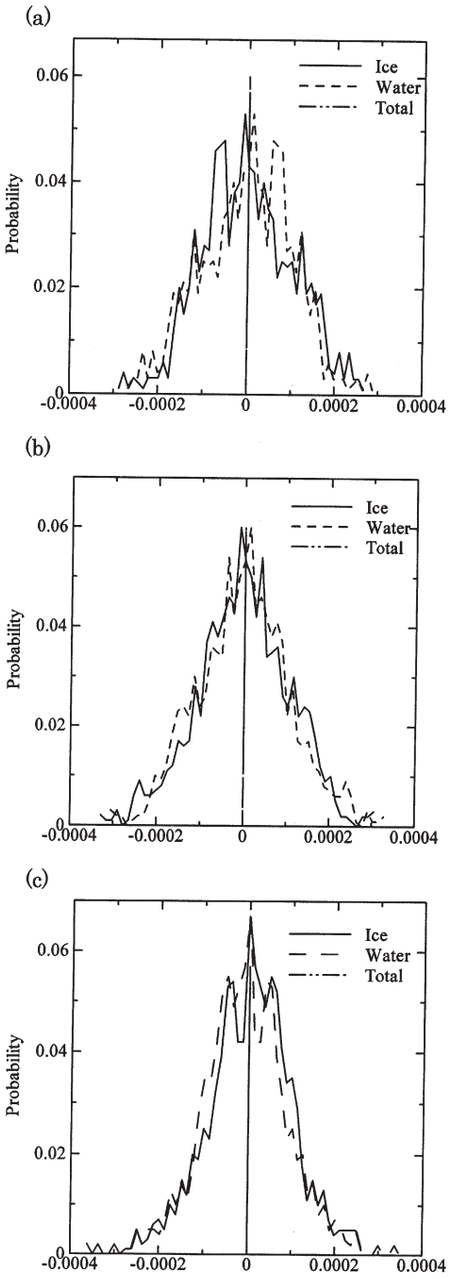

FIGURE 17 Probability density distributions of forces acting on ice and supercooled water (a) x-direction, (b) y-direction (c) z-direction.

receive forces in the positive direction of the x-axis and in the negative directions of the y- and z-axes. The absolute value of the skewness in the y-direction is the lowest among the three.

Figure 18 demonstrates a snapshot of the ice nucleus in the supercooled water from the (x, z)-plane. The nucleus is found to be stretched slightly in the direction of 45° from the horizontal line and squeezed in the direction of 135° from the horizontal line. This shows that the ice nucleus after receiving

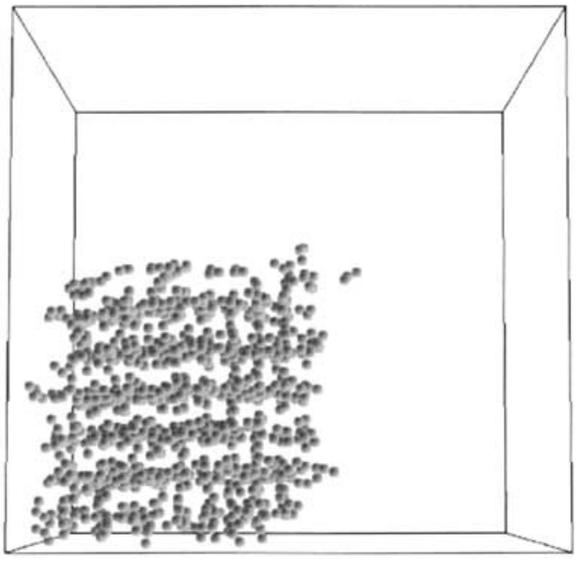

FIGURE 18 Snapshot of the ice in the supercooled water from (x, z)-plane (The hydrogen atoms are omitted).

the force from the water takes not a rectangular but a rhombic shape. This is not contradictory to the forces in Table VI. It should be emphasized that the principal deformation directions are not the same as the directions of crystal growth of ice. This shows anisotropy of ice crystal.

CONCLUSIONS

The molecular dynamics simulation was carried out in order to form ice nucleus and the mixture of ice and water. The main conclusions obtained are as follows.

(1) The ice Ih structure was arranged in the domain of $2.245 \times 2.333 \times 2.200\,\mathrm{nm}^3$ by controlling only the displacements and velocities of 360 water molecules with the condition that the initial location of the center of the molecules was determined from the results in the references.
(2) In order to obtain the ice nucleus surrounded by water in the domain of $4.491 \times 4.667 \times 4.400\,\mathrm{nm}^3$, the energy was given to part of the ice in the domain until the temperature of this part reached the target temperature. The temperature was decided so that the total amount of energy input was approximately equal to the latent heat.
(3) The ice nucleus surrounded by supercooled water was generated from the ice–water mixture at approximately freezing point. The other low target temperature was effective for reducing the energy, which corresponds to the latent heat of solidification.

(4) The power spectra for the ice nucleus and surrounding water showed that the rotational motion is predominant in the high frequency range, which is based on the vibration of hydrogen atoms. The spectra of the translational motion for the nucleus and water were predominant in the mid-frequency range, which is due to the motion of molecules in the liquid region or the deformation of ice due to the anisotropic force. The rotational and transverse motions contributed to the low-frequency range of the spectra. This was caused by the motion of cluster of water molecules and the growth of the ice nucleus.

(5) The ice nucleus took a rhombic structure due to the forces acting on the nucleus.

References

[1] Grandum, S., Yabe, A., Nakagomi, K., Tanaka, M., Takemura, F., Kobayashi, Y. and Frivik, P. (1997) "Microscale analysis of crystals in ice slurry made from an antifreeze protein solution", *Trans. Jpn Soc. Mech. Eng.* **63 Ser. B**, 1029, (in Japanese).

[2] Saito, T., Yabe, A., Inada, T., Zhang, X. and Tanaka, M. (1999) "Microscopic observation of ice crystal surface containing absorbed silane coupling agents", *Trans. Jpn Soc. Mech. Eng.* **65 Ser. B**, 463, (in Japanese).

[3] Karim, O.A. and Haymet, A.D.J. (1988) "The ice/water interface: a molecular dynamics simulation study", *J. Chem. Phys.* **89**, 6889.

[4] Hayward, J.A. and Haymet, A.D.J. (2001) "The ice/water interface: molecular dynamics simulations of the basal, prism, $\{20\bar{2}1\}$ and $\{2\bar{1}\bar{1}0\}$ interfaces of ice Ih", *J. Chem. Phys.* **114**, 3713.

[5] Gay, S.C., Smith, E.J. and Haymet, A.D.J. (2002) "Dynamics of melting and stability of ice Ih: molecular-dynamics simulations of the SPC/E model of water", *J. Chem. Phys.* **116**, 8876.

[6] Svishchev, I.M. and Kusalik, P.G. (1994) "Crystallization of liquid water in a molecular dynamics simulation", *Phys. Rev. Lett.* **73**, 975.

[7] Dalal, P., Knickelbein, J., Haymet, A.D.J., Sönnichsen, F.D. and Madura, J.D. (2001) "Hydrogen bond analysis of type 1 antifreeze protein in water and the ice/water interface", *Phys. Chem. Commun.* **4**, 32.

[8] Hayward, J.A. and Reimers, R. (1997) "Unit cells for the simulation of hexagonal ice", *J. Chem. Phys.* **106**, 1518.

[9] Jorgensen, W.J., Chandrasekhar, J., Madura, J.D., Impey, R.W. and Klein, M.L. (1983) "Simple potential function for water", *J. Chem. Phys.* **77**, 926.

[10] Frenkel, D. and Smit, B. (1996) *Understanding Molecular Simulation* (Academic Press, San Diego).

[11] Gear, C.W. (1971) *Numerical Initial Value Problems in Ordinary Differential Equations* (Prentice-Hall, Englewood Cliffs).

[12] Allen, M.P. and Tildesley, D.J. (1987) *Computer Simulation of Liquid* (Oxford Science, Oxford).

[13] Bolton, K. and Pettersson, J.B.C. (2000) "A molecular dynamics study of long-time ice Ih surface dynamics", *J. Phys. Chem., B* **104**, 1590.

[14] Batista, E.R. and Jónsson, H. (2001) "Diffusion and island formation on the ice Ih basal plane surface", *Comp. Mater. Sci.* **20**, 325.

[15] Mank, V.V. and Levovka, N.I. (1988), Chapter 1, *Spektroskopija jadernogo magnitnogo rezonans vody v geterogennykh sistemakh* (Naukova Dumka, Kiev) **1**.